Biochemical and Biophysical Research Communications 462 (2015) 138–143

Contents lists available at ScienceDirect

Biochemical and Biophysical Research Communications

journal homepage: www.elsevier.com/locate/ybbrc

Pirfenidone enhances the efficacy of combined radiation and sunitinib therapy

Seo-Hyun Choi, Jae-Kyung Nam, Junho Jang, Hae-June Lee*, Yoon-Jin Lee*

Division of Radiation Effects, Korea Institute of Radiological & Medical Sciences, Seoul 139-706, Republic of Korea

ARTICLE INFO

Article history:
Received 13 April 2015
Available online 30 April 2015

Keywords:
Radiotherapy
Sunitinib
Pirfenidone
Lewis lung carcinoma
Transforming growth factor-β

ABSTRACT

Radiotherapy is a widely used treatment for many tumors. Combination therapy using anti-angiogenic agents and radiation has shown promise; however, these combined therapies are reported to have many limitations in clinical trials. Here, we show that radiation transformed tumor endothelial cells (ECs) to fibroblasts, resulting in reduced vascular endothelial growth factor (VEGF) response and increased Snail1, Twist1, Type I collagen, and transforming growth factor (TGF)-β release. Irradiation of radioresistant Lewis lung carcinoma (LLC) tumors greater than 250 mm^3 increased collagen levels, particularly in large tumor vessels. Furthermore, concomitant sunitinib therapy did not show a significant difference in tumor inhibition versus radiation alone. Thus, we evaluated multimodal therapy that combined pirfenidone, an inhibitor of TGF-induced collagen production, with radiation and sunitinib treatment. This trimodal therapy significantly reduced tumor growth, as compared to radiation alone. Immunohistochemical analysis revealed that radiation-induced collagen deposition and tumor microvessel density were significantly reduced with trimodal therapy, as compared to radiation alone. These data suggest that combined therapy using pirfenidone may modulate the radiation-altered tumor microenvironment, thereby enhancing the efficacy of radiation therapy and concurrent chemotherapy.

1. Introduction

Radiotherapy is widely used to treat tumors, including non-small cell lung cancers (NSCLC) [1,2]. However, tumors located in anatomic regions that are difficult to access or adjacent to vital structures have a significant risk of local recurrence. Combined drug therapy can increase the efficacy of radiotherapy by targeting both cancer cells and the microenvironment, including tumor vessels. Anti-angiogenic therapy targets endothelial cells, disrupting the pre-existing tumor vasculature and inhibiting angiogenic vessel formation [1,3]. Sunitinib (Su11248, Sutent) is a multi-target tyrosine kinase inhibitor of the vascular endothelial growth factor receptor (VEGFR1/2/3), platelet-derived growth factor receptor (PDGFRa/b), c-kit, FLT3 and ret. It can inhibit both angiogenesis, by targeting endothelial cells, and tumor growth [4,5]. Preclinical data indicates that sunitinib enhances radiotherapy response [6,7]; however, clinical trials evaluating the efficacy of concurrent sunitinib and radiotherapy are on-going in patients with various cancers, including advanced NSCLC [8].

Combination treatment using anti-VEGF therapy, such as sunitinib, and radiotherapy is limited in dose, treatment schedule, and tumor size [3,9]. *In vivo*, tumor size at therapy onset plays a key role in the efficacy of radiation and anti-VEGF therapy [10]. In several transplantable tumor models, radioresistance emerges when tumors reach approximately 250 mm^3, because critical determinants of radioresistance, including oxygen tension, nutrient supply, and pH, are affected by tumor size [10]. Furthermore, several clinical and experimental reports indicate that smaller initial tumor sizes predict a good response to anti-VEGF therapy [11,12].

In this study, radiotherapy was initiated when Lewis lung carcinoma (LLC) tumors reached sizes greater than 250 mm^3. We examined the efficacy of combined drug treatment on these radioresistant tumors. Previous observations indicate that irradiated normal ECs lose their EC-specific characteristics, becoming fibroblast cells [13]. We hypothesize that radiation changes tumor ECs and the tumor microenvironment. The aim of this study was to better understand the limitations of combined anti-angiogenic and radiation therapy, and to overcome these limitations by modulating the radiation-altered microenvironment.

* Corresponding authors. Fax: +82 2 970 1985.
E-mail addresses: hjlee@kcch.re.kr (H.-J. Lee), yjlee8@kcch.re.kr (Y.-J. Lee).

http://dx.doi.org/10.1016/j.bbrc.2015.04.107
0006-291X/

2. Materials and methods

2.1. Cell culture and treatment

The mouse tumor endothelial cell line 2H11 and mouse LLC cells were purchased from ATCC and cultured in Dulbecco's modified Eagle's medium (DMEM) supplemented with 10% fetal bovine serum (FBS). Cells were exposed to gamma rays derived from a [^{137}Cs] source (Atomic Energy of Canada, Chalk River, Ontario, Canada) at a dose rate of 3.81 Gy/min.

2.2. In vitro tests

Immunoblotting was performed as described previously [14] using antibodies against TGFβ-RI (ALK5), Twist (Santa Cruz Biotechnology, Santa Cruz, CA, USA), p-Smad2/3, Snail1 (Cell Signaling Technology, Beverly, MA, USA), and β-actin (Sigma–Aldrich, St. Louis, MO, USA). For RT-PCR, total RNA was isolated from ECs using TRI reagent (Molecular Research Center, Cincinnati, OH, USA). RNA (1 μg) was used to synthesize cDNA using the Omniscript RT kit (Qiagen, Valencia, CA, USA), followed by amplification using Takara Ex Taq polymerase (Takara Bio Inc., Otsu, Japan). The primer sequences for collagen I transcripts were as follows: forward 5′-CCCAGCTGTCTTATGGCTATGA-3′, reverse 5′-GCACCATCCAAACCACTGAA-3′. A 346 bp band was amplified using the following PCR cycle: initial denaturation 95 °C for 2 min, 35 cycles of 95 °C for 30 s, 58 °C for 30 s, and 72 °C for 45 s, and a final extension at 72 °C for 10 min. Cell proliferation was assessed by 3-(4,5-dimethylthiazol-2-yl)-2,5-diphenyltetrazolium bromide (MTT) assay as described previously [14] Recombinant human $VEGF_{165}$ (R&D Systems, Minneapolis, MN, USA) was used for VEGF-induced proliferation. TGF-β1 released into culture medium was measured using a mouse TGF-β1 enzyme-linked immunosorbent assay (ELISA) kit (Enzo Life Sciences, Farmingdale, NY, USA) according to the manufacturer's instructions.

2.3. In vivo tumor model

All protocols involving mice were approved by the Institutional Animal Care and Use Committee of the Korea Institute of Radiological and Medical Sciences. To generate the syngeneic tumors, 2×10^5 LLC cells were injected subcutaneously into the right thigh of C57BL/6 male mice. Tumors were irradiated when they reached a volume of 250–300 mm^3. Radiation was delivered using an X-RAD 320 (Precision X-ray, North Branford, CT, USA). Sunitinib malate and pirfenidone (Selleckchem, Munich, Germany) were dissolved in DMSO, and were further diluted in 0.3% (w/v) carboxymethyl cellulose (CMC) with 1% (v/v) Tween-80 prior to intraperitoneal injection (40 and 37 mg/kg respectively). Tumor volumes were determined according to the formula $(L \times W \times H)/2$, by measuring tumor length (L), width (W), and height (H) with a caliper. Six mice were used in each group, and tumors were harvested 10 days after irradiation.

2.4. Histology and immunohistochemistry

Mice were euthanized and tumor tissues were harvested and fixed in 10% neutral buffered formalin for paraffin section preparation. Paraffin-embedded tissue sections were deparaffinized and stained as described previously [14]. Tumor vessel density was assessed by CD31 (Abcam, Cambridge, UK) staining. Collagen deposition was assessed using Masson's trichrome staining (Sigma–Aldrich). Collagen positive or CD31 positive areas were evaluated with Image J software. The Student's t-test and analysis of variance (ANOVA) were used to determine statistical significance between experimental groups. Statistical analyses were performed using GraphPad Prism version 5.0 (GraphPad Software).

3. Results

3.1. Radiation altered tumor EC phenotype

Previously, we reported that radiation induces normal aortic EC dysfunction [13]. We assessed phenotypic changes in irradiated tumor ECs. Over 50% of tumor ECs died within 3 days after exposure to 10 Gy irradiation (Fig. 1A). Living tumor ECs underwent morphological changes, displaying irregular, flattened, long, or thinned morphology as shown in Fig. 1B; however, proliferative tumor ECs remained 10 days after irradiation. Furthermore, 10Gy-irradiated tumor ECs did not increase proliferation in the response to VEGF165, whereas the proliferation of non-irradiated tumor ECs increased (Fig. 1C). Tumor ECs displayed increased ALK5, phospho-SMAD2/3, Twist1, and Snail1 expression at the indicated time points following irradiation. RT-PCR analysis also revealed increases in type I collagen gene expression in irradiated tumor ECs 1–4 days after irradiation (Fig. 2A). These results suggest that radioresistant tumor ECs acquire a fibroblast-like phenotype. Since fibroblasts produce various growth factors, including TGF-β, we examined whether radioresistant tumor ECs release TGF-β using an ELISA assay. Irradiated tumor ECs released TGF-β in a dose-dependent manner (Fig. 2B). Together, our data suggest that irradiated tumor ECs have a fibroblast-like phenotype, displaying increased Twist1, Snail1, and type I collagen expression, and TGF-β secretion.

3.2. Pirfenidone increases the efficacy of concurrent sunitinib and radiotherapy

Several groups have reported the effects of combination radiation and anti-angiogenic sunitinib therapy [4,15–17]. We propose that radiation-induced alterations in tumor ECs may limit the effects of sunitinib. Because the altered tumor ECs released TGF-β and increased type I collagen expression, we tested the effects of pirfenidone, an inhibitor of TGF-β-stimulated collagen production, on combination sunitinib and radiation therapy.

The efficacy of radiation and anti-angiogenic therapy is dependent on tumor size [11]. We examined the effects of pirfenidone on combined treatment when tumors reached approximately 300 mm^3. As shown Fig. 3A, at this initial tumor size, radiation does not reduce the LLC tumor size. However, radiation therapy combined with anti-angiogenic sunitinib decreases the growth rate of LLC tumors. The effects of radiation therapy combined with pirfenidone and sunitinib is likely to enhance these effects. Radiation therapy combined with sunitinib and pirfenidone synergistically reduced tumor growth, as compared to combination radiation and sunitinib or pirfenidone (Fig. 3A). A significant ($p < 0.05$) inhibition in tumor growth was observed only when using radiation therapy in combination with both sunitinib and pirfenidone (Fig. 3B).

3.3. Pirfenidone reduces radiation-induced collagen deposition

To test the effects of radiotherapy combined with pirfenidone, we harvested tumors 10 days after radiation and performed Trichrome staining, where blue color indicates collagen deposition. As shown in Fig. 4A, radiation increased collagen deposition around tumor vessels. Compared to combination sunitinib and radiation therapy, pirfenidone reduced radiation-induced collagen deposition. This collagen deposition was primarily affected in large tumor vessels. Next, we tested whether pirfenidone concomitantly affected tumor microvessel density. As shown Fig. 4B, tumor microvessel density was slightly increased 10 days after irradiation

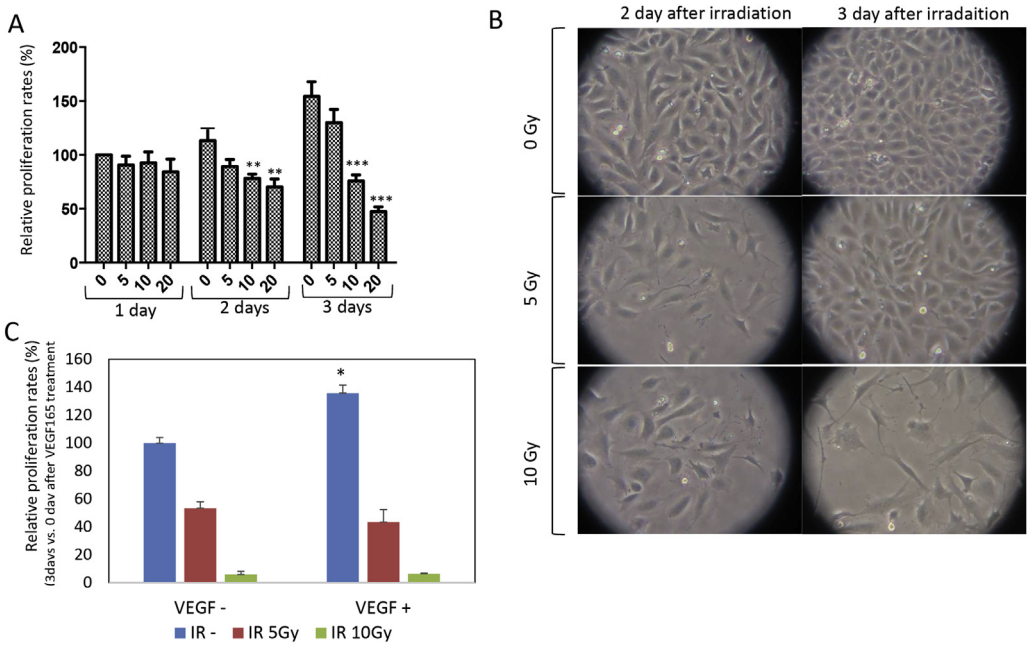

Fig. 1. Radiation changes the characteristics of tumor ECs. (A) Proliferation of 2H11 cells 1, 2 or 3 days after irradiation with 0, 5, 10, or 20 Gy. Error bars indicate SEM. $^{**}P < 0.01$; $^{***}P < 0.001$ vs. no IR. (B) Morphological changes in 2H11 cells 2 or 3 days after irradiation with 0, 5, or 10 Gy. (C) The effect of irradiation on VEGF165-induced 2H11 proliferation. 2H11 cells were irradiated with 0, 5, or 10 Gy, and then cultured with 10 ng/ml VEGF165 10 days after radiation. Proliferation was determined in MTT assays. Error bars indicate SD. $^{*}P < 0.05$ vs. no VEGF (−). Graphs are representative of three independent experiments.

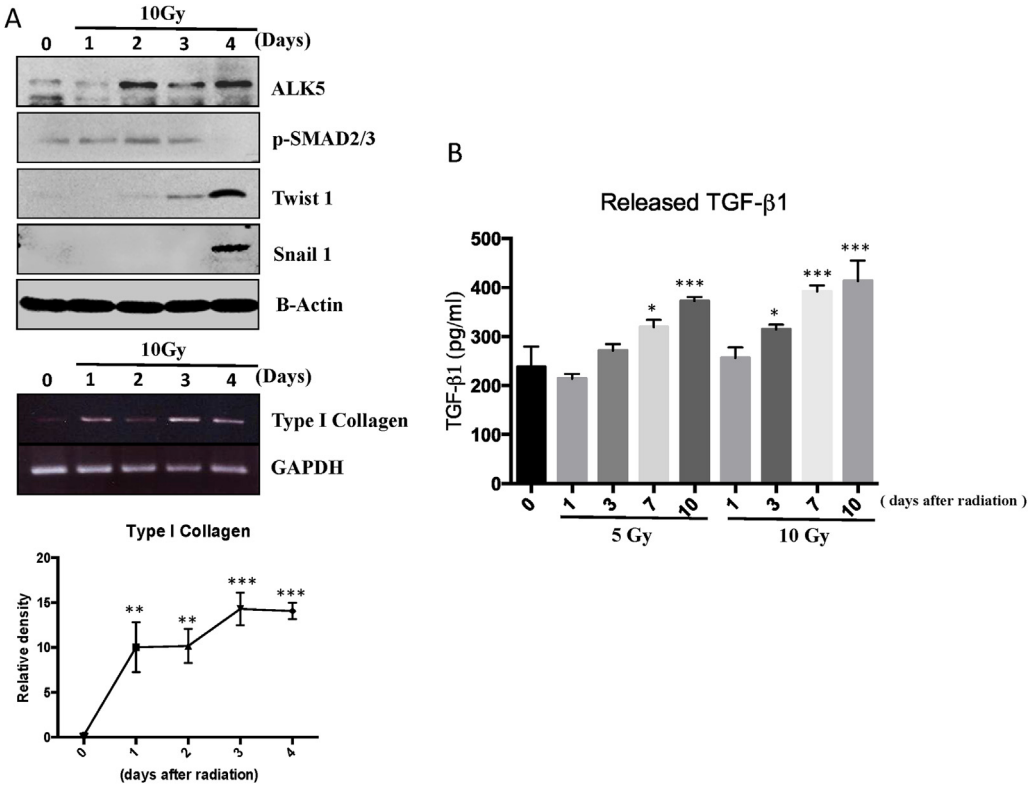

Fig. 2. Radiation increases the expression of fibroblast markers in tumor ECs. (A) Expression of ALK5, Twist1, Snail I, and Collagen I, and phosphorylation of Smad2/3 in irradiated 2H11 cells 0, 1, 2, 3, and 4 days after 10 Gy irradiation were analyzed by Western blot (ALK5, p-Smad2/3, Twist1, Snail I) and RT-PCR (collagen I). Error bars indicate SEM of three independent experiments. $^{**}P < 0.01$; $^{***}P < 0.001$ vs. Control (B) TGF-β1 secretion in irradiated 2H11 cells was determined using ELISA. Error bars indicate SEM of three independent experiments. . $^{*}P < 0.05$; $^{***}P < 0.001$ vs. Control.

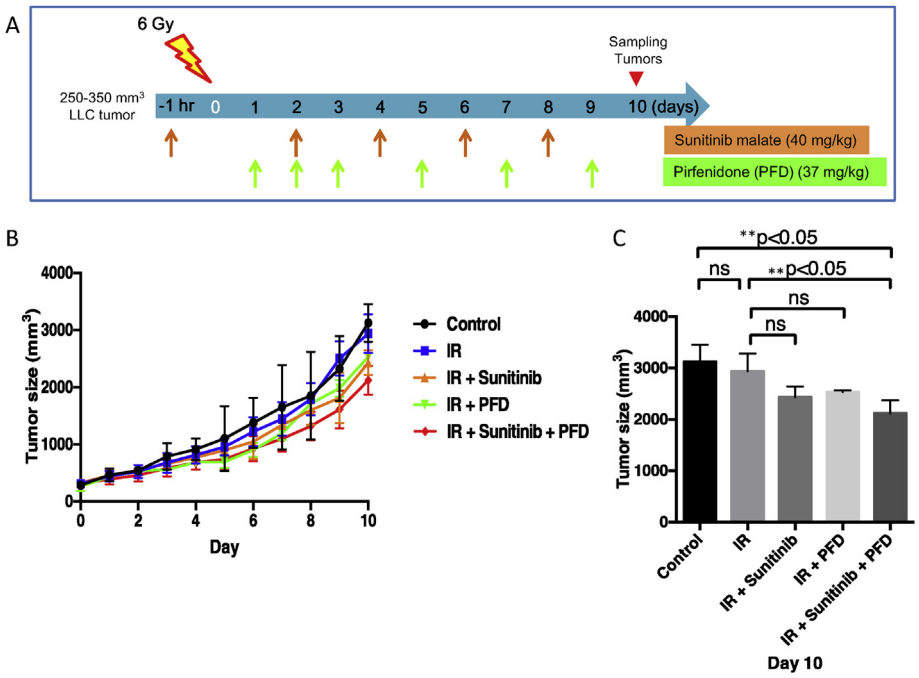

Fig. 3. Combination treatment using sunitinib malate and pirfenidone (PFD) increases the radiosensitivity of tumors *in vivo*. (A) Experimental protocol for combination therapy. Administration of sunitinib malate was started 1 h before irradiation (6 Gy) and continued once every 2 days for 8 days at a dose of 40 mg/kg. Administration of PFD was initiated 1 day after irradiation and continued once daily for 3 days and once every 2 days for 6 days at a dose of 37 mg/kg. (B) Tumor growth was monitored every day for 10 days after irradiation. ($n = 6$) (C) Tumor volumes on day 10 after irradiation. Error bars indicate SD. Graphs are representative of two independent experiments.

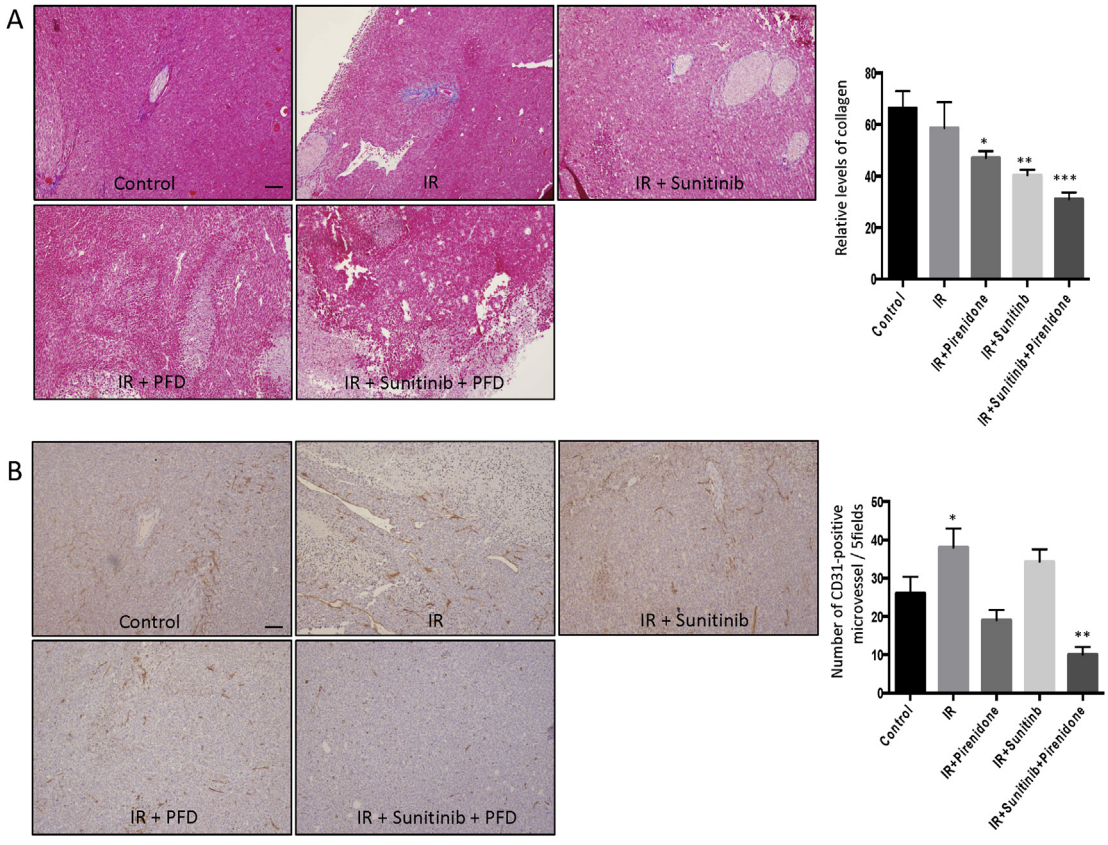

Fig. 4. Reduced collagen deposition and vessel density in tumor tissues after combination therapy using sunitinib malate, pirfenidone (PFD), and radiation. (A) Masson's trichrome staining of LLC tumor tissues collected 10 days after 6 Gy irradiation. Collagen is stained blue, nuclei purple, and cytoplasm red/pink. The original magnification was 200×. Scale bar = 100 μm. The graph shows the relative levels of collagen in tumors, as the average of the five 100 × fields (error bars indicate the SEMs with six mice per group; $^{*}P < 0.05$; $^{**}P < 0.01$; $^{***}P < 0.001$ vs. Control) (B) Vessel density of LLC tumor tissues collected 10 days after 6 Gy irradiation. Endothelial cell marker CD31 stained brown. The original magnification was 200×. Scale bar = 100 μm. The graph shows the average number of CD31-labeled microvessels in the five 200× fields/tumor. (Error bars indicate the SEMs with six mice per group; $^{*}P < 0.05$; $^{**}P < 0.01$; $^{***}P < 0.001$ vs. Control). (For interpretation of the references to color in this figure legend, the reader is referred to the web version of this article.)

alone, as compared to control tumors. Radiotherapy combined with sunitinib reduced microvessel density; however, large tumor vessels were still observed, as compared to tumor microvessels. Furthermore, combined treatment with pirfenidone significantly reduced tumor microvessel intensity, accompanied with a reduction in large tumor vessels. Together, these data suggest that pirfenidone reduces radiation-induced collagen deposition. Thus, radiation alone or radiation therapy combined with sunitinib has synergistic anti-tumor effects in combination with pirfenidone.

4. Discussion

There is an increasing interest in combination radiation and anti-angiogenic drug therapy for various cancer patients. However, recent reports indicate that the efficacy of these combinations depends on the dose and treatment schedule [15,16,18]. Recent datas suggest that concurrent sunitinib and radiotherapy is a promising treatment for cancer patients, because sunitinib inhibits both angiogenesis and tumor growth [7,17,19]. However, these data are controversial.

We found that radiation induced phenotypic changes in tumor ECs, inducing tumor EC radioresistance and inhibiting response to VEGF. Moreover, tumor ECs had a fibroblast-like phenotype following irradiation, increasing collagen levels and the secretion of TGF-β. Thus, we propose that radioresistant tumor ECs undergoing radiotherapy are not affected by anti-angiogenic therapy targeting EC-specific VEGF or VEGFR1/2. Thus, we suggest that a multimodal therapy that targets a regulator of tumor EC phenotypic changes may increase the efficacy of combination therapy. Indeed, in large LLC tumors that underwent radiotherapy, collagen deposition was increased, especially around tumor vessels, as compared to control tumors. As expected, combination radiation, sunitinib, and pirfenidone, an inhibitor TGF-β-stimulated collagen production, therapy reduced radiation-induced collagen deposition and LLC tumor growth. Radiation and pirfenidone or radiation and sunitinib delayed LLC tumor growth; however, maximal growth inhibition and reduced microvessel density was observed using all three.

Supporting our data, there are many reports that TGF-β is a major regulator of radiation sensitivity [20,21]. Additionally, several reports indicate that tumor formation and metastasis are related to increased tumor stromal collagen [22–24]. A recent study reported that collagen VI is a potent biomarker of chemotherapy resistance [25].

Radiation-induced phenotypic changes in tumor ECs and collagen deposition around tumor vessels may lead to fibroblast proliferation and changes in the tumor microenvironment after radiation. Resistance to chemo- or radiotherapy is associated with cancer fibroblasts [26,27]. Furthermore, it has been reported that cancer-associated fibroblasts do not respond to combined irradiation and kinase inhibitors [28].

Additionally, radiation-induced pulmonary fibrosis (RIPF) is a major late side effect following radiation therapy in lung cancer patients [29–31]. Pirfenidone was originally an anti-fibrotic drug for the treatment of idiopathic pulmonary fibrosis (IPF), via regulation of TGF-β and procollagen I and II production [32–35]. Therefore, we are further studying whether pirfenidone has effects on radiotherapy for lung cancer accompanied by RIPF. Our data indicate that targeting radiation-induced changes in tumor ECs may enhance the efficacy of radiation therapy or combination therapy using radiation and anti-angiogenic drugs.

Conflict of interest

The authors declare no conflicts of interest related to this work.

Acknowledgments

This work was supported by the Nuclear Research and Development Program (grant nos. NRF-2011-0031697, NRF-2013M2A2A7043580 and NRF-2014M2A2A7044825) through the National Research Foundation of Korea, funded by the Ministry of Science, Information, and Communications Technology, and Future Planning.

Transparency document

Transparency document related to this article can be found online at http://dx.doi.org/10.1016/j.bbrc.2015.04.107.

References

[1] T. Le Chevalier, R. Arriagada, E. Quoix, et al., Radiotherapy alone versus combined chemotherapy and radiotherapy in nonresectable non-small-cell lung cancer: first analysis of a randomized trial in 353 patients, J. Natl. Cancer Inst. 83 (1991) 417–423.
[2] A.W. Goolden, Radiation cancer: a review with special reference to radiation tumours in the pharynx, larynx, and thyroid, Br. J. Radiol. 30 (1957) 626–640.
[3] E.A. Kleibeuker, M.A. Ten Hooven, K.C. Castricum, et al., Optimal treatment scheduling of ionizing radiation and sunitinib improves the antitumor activity and allows dose reduction, Cancer Med. (2015 Mar 31), http://dx.doi.org/10.1002/cam4.441 [Epub ahead of print]. PMID: 25828633.
[4] S. Faivre, G. Demetri, W. Sargent, et al., Molecular basis for sunitinib efficacy and future clinical development, Nat. Rev. Drug. Discov. 6 (2007) 734–745.
[5] M.A. Socinski, The current status and evolving role of sunitinib in non-small cell lung cancer, J. Thorac. Oncol. 3 (2008) S119–S123.
[6] J. Kao, C.T. Chen, C.C. Tong, et al., Concurrent sunitinib and stereotactic body radiotherapy for patients with oligometastases: final report of a prospective clinical trial, Target Oncol. 9 (2014) 145–153.
[7] C.C. Tong, E.C. Ko, M.W. Sung, , et al.J. Kao, Phase II trial of concurrent sunitinib and image-guided radiotherapy for oligometastases, PLoS One 7 (2012) e36979.
[8] C. Nieder, N. Wiedenmann, N.H. Andratschke, et al., Radiation therapy plus angiogenesis inhibition with bevacizumab: rationale and initial experience, Rev. Recent Clin. Trials 2 (2007) 163–168.
[9] T.Y. Seiwert, J.K. Salama, E.E. Vokes, The concurrent chemoradiation paradigm-general principles, Nat. Clin. Pract. Oncol. 4 (2007) 86–100.
[10] P. Wachsberger, R. Burd, A.P. Dicker, Tumor response to ionizing radiation combined with antiangiogenesis or vascular targeting agents: exploring mechanisms of interaction, Clin. Cancer Res. 9 (2003) 1957–1971.
[11] E.J. Abel, S.H. Culp, N.M. Tannir, et al., Early primary tumor size reduction is an independent predictor of improved overall survival in metastatic renal cell carcinoma patients treated with sunitinib, Eur. Urol. 60 (2011) 1273–1279.
[12] C. Seidel, M. Fenner, A.S. Merseburger, et al., Response of renal lesions during systemic treatment with sunitinib in patients with metastatic renal cell carcinoma: a single center experience with 14 patients, World J. Urol. 29 (2011) 355–360.
[13] M. Kim, S.H. Choi, Y.B. Jin, et al., The effect of oxidized low-density lipoprotein (ox-LDL) on radiation-induced endothelial-to-mesenchymal transition, Int. J. Radiat. Biol. 89 (2013) 356–363.
[14] Y.J. Lee, H.J. Lee, S.H. Choi, et al., Soluble HSPB1 regulates VEGF-mediated angiogenesis through their direct interaction, Angiogenesis 15 (2012) 229–242.
[15] L.Q. Chow, S.G. Eckhardt, Sunitinib: from rational design to clinical efficacy, J. Clin. Oncol. 25 (2007) 884–896.
[16] A. Prasanna, M.M. Ahmed, M. Mohiuddin, et al., Exploiting sensitization windows of opportunity in hyper and hypo-fractionated radiation therapy, J. Thorac. Dis. 6 (2014) 287–302.
[17] A.J. Schueneman, E. Himmelfarb, L. Geng, et al., SU11248 maintenance therapy prevents tumor regrowth after fractionated irradiation of murine tumor models, Cancer Res. 63 (2003) 4009–4016.
[18] J. Kao, S. Packer, H.L. Vu, et al., Phase 1 study of concurrent sunitinib and image-guided radiotherapy followed by maintenance sunitinib for patients with oligometastases: acute toxicity and preliminary response, Cancer 115 (2009) 3571–3580.
[19] R.J. Motzer, T.E. Hutson, P. Tomczak, et al., Sunitinib versus interferon alfa in metastatic renal-cell carcinoma, N. Engl. J. Med. 356 (2007) 115–124.
[20] S. Biswas, M. Guix, C. Rinehart, et al., Inhibition of TGF-beta with neutralizing antibodies prevents radiation-induced acceleration of metastatic cancer progression, J. Clin. Invest 117 (2007) 1305–1313.
[21] H.C. Dancea, M.M. Shareef, M.M. Ahmed, Role of radiation-induced TGF-beta signaling in Cancer therapy, Mol. Cell. Pharmacol. 1 (2009) 44–56.
[22] D.M. Gilkes, S. Bajpai, C.C. Wong, et al., Procollagen lysyl hydroxylase 2 is essential for hypoxia-induced breast cancer metastasis, Mol. Cancer Res. 11 (2013) 456–466.
[23] D.M. Gilkes, P. Chaturvedi, S. Bajpai, et al., Collagen prolyl hydroxylases are essential for breast cancer metastasis, Cancer Res. 73 (2013) 3285–3296.

[24] P. Lu, V.M. Weaver, Z. Werb, The extracellular matrix: a dynamic niche in cancer progression, J. Cell. Biol. 196 (2012) 395–406.
[25] P. Chen, M. Cescon, P. Bonaldo, Collagen VI in cancer and its biological mechanisms, Trends Mol. Med. 19 (2013) 410–417.
[26] M. Loeffler, J.A. Kruger, A.G. Niethammer, et al., Targeting tumor-associated fibroblasts improves cancer chemotherapy by increasing intratumoral drug uptake, J. Clin. Invest. 116 (2006) 1955–1962.
[27] F. Lotti, A.M. Jarrar, R.K. Pai, et al., Chemotherapy activates cancer-associated fibroblasts to maintain colorectal cancer-initiating cells by IL-17A, J. Exp. Med. 210 (2013) 2851–2872.
[28] A. Affolter, I. Schmidtmann, W.J. Mann, et al., Cancer-associated fibroblasts do not respond to combined irradiation and kinase inhibitor treatment, Oncol. Rep. 29 (2013) 785–790.
[29] R.A. Rosiello, W.W. Merrill, Radiation-induced lung injury, Clin. Chest Med. 11 (1990) 65–71.
[30] C. Chargari, F. Riet, M. Mazevet, et al., Complications of thoracic radiotherapy, Presse. Med. 42 (2013) e342–351.
[31] J.N. Finkelstein, C.J. Johnston, R. Baggs, et al., Early alterations in extracellular matrix and transforming growth factor beta gene expression in mouse lung indicative of late radiation fibrosis, Int. J. Radiat. Oncol. Biol. Phys. 28 (1994) 621–631.
[32] B.A. Karimi-Shah, B.A. Chowdhury, Forced vital capacity in idiopathic pulmonary fibrosis–FDA review of pirfenidone and nintedanib, N. Engl. J. Med. 372 (2015) 1189–1191.
[33] E.S. Kim, G.M. Keating, Pirfenidone: a review of its use in idiopathic pulmonary fibrosis, Drugs 75 (2015) 219–230.
[34] P. Spagnolo, N. Sverzellati, G. Rossi, et al., Idiopathic pulmonary fibrosis: an update, Ann. Med. 47 (2015) 15–27.
[35] K. Togami, A. Miyao, K. Miyakoshi, et al., Efficient delivery to human lung fibroblasts (WI-38) of pirfenidone incorporated into liposomes modified with truncated basic fibroblast growth factor and its inhibitory effect on collagen synthesis in idiopathic pulmonary fibrosis, Biol. Pharm. Bull. 38 (2015) 270–276.